Radial Velocity Study

C. Mansperger

Motivated by the claims of Stickland (1989) and Thompson (1990) on the radial velocities as derived by IUE, a study is in progress to determine whether there is any correlation between radial velocities measured from IUE high dispersion spectra and the date of processing. Thus far, two PHCAL standard stars, three radial velocity standard stars, and RR Tel have been used for this purpose. Information on these stars is given in Table I.

Table I

HD #	Name	Spec Type	RV (k/s)	Vsini (k/s)	Distance (pc)
34816	λ Lep	B0 IV	+20.0[a]	50[b]	501[c]
3360	ζ Cas	B2 IV	−6[d]	18[e]	250[e]
	RR Tel		−61.8[f]		
108903		F0 IV	+21.3[g]		
144579		dG8	−60.0[g]		
171232		G8 III	−35.9[g]		

[a] McNamara and Hansen (1961)
[b] Uesugi (1982)
[c] Bohlin *et al.* (1983)
[d] Heckathorn (1983)
[e] Hoffleit (1982)
[f] GCRV
[g] Nautical Almanac

The first star used for this study is λ Lep which has a radial velocity of 20.0 km/sec. There is no evidence that this radial velocity varies. The Mg II 2802 absorption line was measured from 25 LWP images taken between October, 1982

and February, 1991. The absorption lines were measured with the RDAF routines FEATURE and GAUSSFITS. The radial velocities from both of these methods were then plotted versus processing date. A line was fit through each set of radial velocities. These fits are shown in Figures 1 and 2 and the results of the fits are given in Table II. Clearly this shows no correlation between measured radial velocities and processing date. The mean radial velocity from FEATURE was 27 km/sec, and the mean radial velocity from GAUSSFITS was 26 km/sec. This is higher than one would expect from interstellar absorption lines.

The interstellar absorption lines S II 1259, Si II 1260 and S II 1251 were then measured for λ Lep from 19 SWP images. These images were processed between November 18, 1981 and February, 1991. The results are also given in Table II. The fits are shown in Figures 3 thru 5.

Table II

Line	Method	Slope	Cor. coef.	Mean RV (k/s)
Mg II 2802	FEATURE	-0.08 ± 0.08	-0.05	27.
Mg II 2802	GAUSSFITS	$+0.04 \pm 0.08$	0.04	26.
Si II 1260	GAUSSFITS	$+1.25 \pm 0.07$	0.80	6.5
S II 1259	GAUSSFITS	$+1.42 \pm 0.08$	0.80	11.9
S II 1251	GAUSSFITS	$+1.57 \pm 0.08$	0.84	14.1
Si II 1260[a]	GAUSSFITS	$+1.18 \pm 0.08$	0.75	5.7
S II 1259[a]	GAUSSFITS	$+1.36 \pm 0.08$	0.77	11.1

[a] Heliocentric velocity correction from IUEVEL

The Si II and S II absorption lines do indeed indicate that there is a correlation between processing date and the derived radial velocity. All of the λ Lep SWP images had a heliocentric velocity correction applied to them by IUESIPS at the time they were processed. The IUESIPS' correction for spacecraft motion uses a set of orbital elements from 1979 to calculate IUE's contribution to the velocity vector

rather than the current elements as of the time of the observations. To determine if this was causing the trend of increasing radial velocities, this correction was removed from all of the λ Lep SWP images. The RDAF routine IUEVEL, which uses orbital elements current as of the time of observations, was then used to determine the heliocentric velocity correction for all these images. Gaussian fits were then made to the Si II 1260 and S II 1259 absorption lines present in the images with the IUEVEL correction. Figures 6 and 7 and Table II show the results. Using the IUEVEL correction did not eliminate the trend of increasing radial velocities with processing date. The biggest difference between a radial velocity derived from an image with the IUEVEL correction to that of a radial velocity derived from an image with the IUESIPS correction was 2 km/sec.

The interstellar Mg II 2802 absorption line which is present in the spectrum of ζ Cas was measured from 17 LWP images. These images were processed between January, 1982 and July, 1990. These absorption lines were also measured with both FEATURE and GAUSSFITS. Also, the interstellar absorbtion lines Si II 1260, and S II 1259 were measured from 19 SWP images of ζ Cas. These images were processed between May, 1980 and September, 1991. IUEVEL was used to correct for the heliocentric velocity for those images which were processed before November, 1981 when IUESIPS began to apply this correction. The radial velocities from these measurements were also plotted versus processing date, and a line was fit through each of these plots. The results are shown in Table III and Figures 8 thru 13.

Table III

Line	Method	Slope	Cor. coef.	Mean RV (k/s)
Mg II 2802	FEATURE	$+0.13 \pm 0.09$	0.08	8.6
Mg II 2802	GAUSSFITS	$+0.29 \pm 0.09$	0.19	8.9
Si II 1260	FEATURE	$+0.57 \pm 0.07$	0.36	-5.4
Si II 1260	GAUSSFITS	$+0.44 \pm 0.07$	0.29	-4.6
S II 1259	FEATURE	$+0.43 \pm 0.07$	0.32	-8.6
S II 1259	GAUSSFITS	$+0.44 \pm 0.07$	0.33	-6.8

While all of the lines fit to radial velocity versus processing date for ζ Cas show a positive slope, the correlation coefficients are still closer to 0 than to 1. Note that the mean radial velocity for the interstellar absorption line Mg II 2802 is ~ 9 km/sec. One would expect radial velocities measured from interstellar absorption lines to be closer to 0. Again, it appears that radial velocities measured from LWP absorption lines are larger than expected. Note, also, that from Tables II and III it appears that the radial velocities derived from absorption lines present in LWP images are on average $\sim$ 15 km/sec larger than those derived from absorption lines present in SWP images. This may be due to the fact that different species of lines were measured from spectra taken with the two different cameras. However, Nichols-Bohlin and FESEN (1986; 1990) found an average difference of 17 km/sec between radial velocities derived from LWR spectra and radial velocities derived from SWP spectra for 19 stars in the line of sight to HD 50896. This study included Fe II 1608, Fe II 2599, and Fe II 2382. This is very similar to the differences between radial velocities derived from LWP spectra and radial velocities derived from SWP spectra found in this study.

The widths and strengths of the S II 1259 and Si II 1260 absorption lines are very similar in both λ Lep and ζ Cas. Their FWHM range from .1 - .2 Å. Their strengths range from $2-3 \times 10^{-9} erg/cm^2/s$. The only obvious difference between the two data sets is that for λ Lep no images were used which were processed before November 10, 1981. As mentioned above, it was on this date IUESIPS began to

apply a correction for spacecraft motion to high dispersion spectra. As an exercise, the three ζ Cas images which were processed before this date were excluded from the fit. The results are shown in Table IV and Figures 14 thru 17.

Table IV

Line	Method	Slope	Cor. coef.	Mean RV (k/s)
Si II 1260	GAUSSFITS	$+1.13 \pm 0.08$	0.69	-5.3
Si II 1260	FEATURE	$+1.14 \pm 0.08$	0.65	-5.9
S II 1259	GAUSSFITS	$+1.01 \pm 0.08$	0.67	-7.3
S II 1259	FEATURE	$+1.03 \pm 0.08$	0.67	-9.2

This indicates there is a weak correlation between radial velocity and processing date. However, this trend did not begin until after November 10, 1981. Also, the slopes of these linear fits are very similar to those from the λ Lep data. It would be unlikely that both of these standard stars are varying in radial velocity by the same degree in the same direction.

All of the interstellar lines in ζ Cas and the Mg II line in λ Lep were fit with both FEATURE and GAUSSFITS to determine if the method of fit would effect any trends which are present. Regardless of which fitting routine was used the same trends, or lack thereof, were present. Therefore, it was deemed unnecessary to continue using both fitting routines. The plots from gaussian fits show less scatter. Also, GAUSSFITS seemed more robust than FEATURE. It produced the same results regardless of the input from the user. FEATURE's results seem more sensitive to input from the user. For the remainder of the study only GAUSSFITS was used for measuring lines.

The third object of this study is RR Tel which has a radial velocity of -61.8 km/sec. Three emission lines, He II 2733, He II 2511, and Fe II 2508 were measured from six LWP images taken from March, 1984 to July, 1992. The results are shown in Table V and Figure 18. Again the radial velocities show no trend with time. However, the average radial velocity derived from these lines is $\sim$ 16 km/sec large

than the known radial velocity of the system. N V 1242, Si IV 1394 and 1403, and C IV 1551 were measured in six SWP images taken between October, 1982 and July 1992. C IV was slightly over exposed in these images. The results also are shown in Table V and in Figure 19. As in λ Lep and ζ Cas there is an increase in radial velocity with time.

Table V

Line	Method	Slope	Cor. coef.	Mean RV (k/s)
N V 1242	GAUSSFITS	$+2.14 \pm 0.11$	0.90	-50
Si IV 1394	GAUSSFITS	$+2.31 \pm 0.11$	0.93	-47
Si IV 1403	GAUSSFITS	$+1.77 \pm 0.11$	0.82	-47
C IV 1551	GAUSSFITS	$+2.09 \pm 0.11$	0.94	-47
He II 2733	GAUSSFITS	$+0.12 \pm 0.14$	0.21	-42
He II 2511	GAUSSFITS	-0.20 ± 0.14	-0.17	-48
Fe II 2508	GAUSSFITS	$+0.19 \pm 0.14$	0.25	-48

To further this study HD 108903, which is a radial velocity standard star, was observed with IUE. This object has a radial velocity of $+21.3 \pm 0.1$ according to the 1992 Astronomical Almanac. The observation of this object was made in March, 1992. The data was processed shortly after. The fits made to the λ Lep and ζ Cas data sets suggest that radial velocities derived from SWP images have increased by $\sim 1.6 \pm .7$ km/sec since 1981. If this is true then radial velocities measured from images processed in 1992 should be 10 to 25 km/sec greater than expected. (e.g. Radial velocities from an image of HD 108903 processed in 1992 should be between +31 and +46 km/sec.) O I 1304, O I 1306, and C I 1656 emission were present in the image of HD 108903. Interstellar absorption lines were superimposed on these emission lines. For this reason the cores of the emission lines were excluded from the gaussian fits which were made to them. The radial velocities derived from the O I 1304 and O I 1306 emission lines were +44 km/sec and +40 km/sec respectively. The radial velocity derived from C I 1656 was +39 km/sec. These values are consistent with the prediction.

The radial velocity standards HD 144579 and HD 171232 were observed with the LWP camera. HD 144579 has a radial velocity of -60.0 ± .3 km/sec according to the Astronomical Almanac. The emission lines Al II 2660 and Mg II 2802 were present in the LWP spectrum. From these lines radial velocities of -46 and - 43 were derived. The radial velocity of HD 171232 is -35.9 ± .5 km/sec. From the Mg II 2802 emission line a radial velocity of -21 km/sec was measured. Both of these cases indicate that the radial velocities found from LWP images are $\sim$ 15 km/sec larger than expected.

The difference between the radial velocities measured from S II 1259 and Si II 1260 were plotted versus processing date for both ζ Cas and λ Lep. These are shown in Figures 20 thru 24. In ζ Cas the Si II 1260 absorption line consistently resulted in a radial velocity $\sim$ 2 - 3 km/sec higher than that measured from the S II 1259 line. However, there does not appear to be any correlation between this difference and the processing date. When the images processed before November, 1981 were dropped from the fit, there was little change in the resulting slope or correlation coefficient. In λ Lep, Si II 1260 on average resulted in a radial velocity which was 5 km/sec less than that measured from S II 1259. Again, there was no significant correlation between this difference and the processing date. The results of the fits are given in Table VI.

Table VI

Star	Method	Slope	Cor. coef.	Mean Δ RV
ζCas^a	GAUSSFITS	-0.01 ± 0.07	-0.01	2.2
ζCas^a	FEATURE	$+0.14 \pm 0.07$	0.16	3.2
ζCas^b	GAUSSFITS	$+0.12 \pm 0.08$	0.23	2.0
ζCas^b	FEATURE	$+0.11 \pm 0.08$	0.12	3.3
λ Lep	GAUSSFITS	-0.16 ± 0.08	-0.39	-5.4

[a] Fit made to complete data set.

[b] Images processed before 11/10/81 excluded from fit.

It is not surprizing that there is a difference in radial velocities measured from Si II 1260 and those measured from S II 1259. This is seen in many spectra. The Si II line is often blended with C I and there may be a problem with the laboratory measurements of the S II lines (Nichols-Bohlin 1992). The purpose of making the comparison between the lines was to see if this difference varied with processing date, which it did not. If the difference in radial velocities had increased or decreased with time, then this may have helped us to understand what was causing the trend of increasing radial velocities.

The dispersion constants for all cameras are occasionally updated. Table VII gives the dates which new dispersion constants were implemented and the corrections that were applied for each camera.

Table VII

Camera	Implementation Date	Corrections Applied	Reference
LWR	7-18-80	none	1
	4-30-81	none	2
	5-19-81	THDA & Time	2
	9-21-82	THDA & Time	3
	6-20-84	THDA & 2nd Order Time	5
	4-01-88	THDA & 2nd Order Time	6
SWP	7-18-80	none	1
	4-30-81	none	2
	5-19-81	THDA & Time	2
	9-21-82	THDA & Time	3
	6-20-84	THDA & 2nd Order Time	6
	4-01-88	THDA & 2nd Order Time	6
LWP	8-17-81	none	
	9-21-82	none	3
	4-12-83	THDA	4
	6-20-84	THDA	5
	4-01-88	THDA	6

1) Thompson, *et al.* (1980)
2) Thompson, Turnrose and Bohlin (1982)
3) Thompson and Turnrose (1983)
4) Thompson (1983)
5) Gass and Thompson (1984)
6) Thompson (1988a)

From the plots of radial velocities derived from SWP images versus processing date it appears that the trend doesn't really begin until around 1984. New dispersion coefficient were implemented on June 20, 1984. Therefore, separate fits were made to the data processed between November 10, 1981 and June 20, 1984 and the data processed after June 20, 1984. The results are shown in Table VIII and in Figures 25 thru 29.

Table VIII

Star	Line	Slope	Cor. coef.	Mean RV (k/s)
ζCas^a	Si II 1260	-0.38 ± 0.66	-0.09	-8.0
ζCas^b	Si II 1260	$+1.93 \pm 0.15$	+0.77	-4.0
ζCas^a	S II 1259	-0.59 ± 0.66	-0.16	-10.0
ζCas^b	S II 1259	$+1.60 \pm 0.15$	+0.70	-6.1
λLep^a	Si II 1260	-2.09 ± 0.50	-0.58	2.8
λLep^b	Si II 1260	$+1.92 \pm 0.11$	+0.94	7.1
λLep^a	S II 1259	-1.75 ± 0.50	-0.43	8.0
λLep^b	S II 1259	$+2.19 \pm 0.11$	+0.95	12.5
λLep^a	S II 1251	-0.85 ± 0.50	-0.21	9.1
λLep^b	S II 1251	$+1.94 \pm 0.11$	0.91	15.4

[a] Fit made to data processed between 11/10/81 and 6/20/84

[b] Fit made to data processed after 6/20/84

From Table VIII it is quite clear that the trend of increasing radial velocity with processing date does not begin until after the dispersion constant implementation of 1984. The SWP constants contain a second order time correction. It has been discovered that this correction can cause a shift in radial velocities with time. Before the last implementation of dispersion constants it was discovered that radial velocities from SWP images had shifted by 3 km/sec (Thompson 1988b). Last year it was determined that the radial velocities had shifted by 12 km/sec since the latest implementation (Garhart 1991). This second order time correction is not applied to the LWP dispersion constants. This may explain why the same trend is not seen

in the LWP data as in the SWP. An experimental version of the RDAF routine, DCCOR was created to correct for the shift introduced by the second order time correction in SWP high dispersion images taken after June 20, 1984. This routine was run on all the λ Lep and all the ζ Cas SWP images. Also, IUEVEL was used to made the heliocentric correction. The results are shown in Table IX and in Figures 30 thru 34.

Table IX

Star	Line	Slope	Cor. coef.	Mean RV (k/s)
ζCas^a	Si II 1260	$+0.28 \pm 0.08$	+0.25	-8.1
ζCas^a	S II 1259	$+0.13 \pm 0.08$	+0.12	-10.2
ζCas^b	Si II 1260	$+0.43 \pm 0.08$	+0.40	-7.3
ζCas^b	S II 1259	$+0.35 \pm 0.08$	+0.35	-9.5
λLep^a	Si II 1260	$+0.40 \pm 0.08$	+0.43	3.7
λLep^a	S II 1259	$+0.57 \pm 0.08$	+0.51	9.1
λLep^a	S II 1251	$+0.72 \pm 0.08$	+0.62	11.2
λLep^b	Si II 1260	$+0.33 \pm 0.08$	+0.33	2.9
λLep^b	S II 1251	$+0.53 \pm 0.08$	+0.46	10.3
λLep^b	S II 1259	$+0.48 \pm 0.08$	+0.42	8.2
$\zeta Cas^{b,c}$	Si II 1260	$+0.91 \pm 0.15$	+0.54	-7.0
$\zeta Cas^{b,c}$	S II 1259	$+0.69 \pm 0.15$	+0.42	-9.2
$\lambda Lep^{b,c}$	Si II 1260	$+0.87 \pm 0.14$	+0.67	3.2
$\lambda Lep^{b,c}$	S II 1251	$+1.12 \pm 0.14$	0.75	8.6
$\lambda Lep^{b,c}$	S II 1259	$+1.01 \pm 0.14$	+0.63	10.8

[a] Heliocentric correction made with IUESIPS.

[b] Heliocentric correction made with IUEVEL.

[c] Images processed before 6/20/84 are excluded from the fit.

In the case of λ Lep using IUEVEL helped to diminish the trend, but in the case of ζ Cas using IUEVEL made things worse. Hence, it seems that while using the wrong Heliocentric correction can lead to a systematic error which contributes

to this effect, it may not. It may even lead to a systematic error which diminishes the effect. This explains why the λ Lep data had higher correlation coefficient and slopes than ζ Cas data did. Indeed, after both corrections are made to both stars the correlation coefficients and slopes are very similar:

$$\text{slope} = +0.4 \pm 0.2 \text{ km/sec/year}$$
$$\text{correlation coefficient} = +0.4 \pm 0.1$$

While a single fit with a correlation coefficient of 0.4 would indicate there was no trend present, five fits with this correlation coefficient and the same slope seem significant. When the data taken only after June 20, 1984 is considered the remains of the trends are even more apparent (Figures 35 thru 39). The average slope and correlation coefficient are:

$$\text{slope} = +0.9 \pm 0.2 \text{ km/sec/year}$$
$$\text{correlation coefficient} = +0.6 \pm 0.2$$

If the derived radial velocity from SWP images has been increasing by .9 ±.2 km/sec/year since 1984, then a radial velocity from an image processed in 1992 should be 5.6 to 8.8 km/sec greater than expected. Therefore, radial velocities from the DCCOR corrected image of HD 108903 should be between 26.9 and 30.1 km/sec. Indeed the radial velocities measured from O I 1304, O I 1306, and C I 1656 are 34, 30 and 29 km/sec respectively. Therefore, while the second order time correction and in some cases the heliocentric correction applied by IUESIPS seem to be contributing to the trend of increasing radial velocity with processing date there appears to be another unknown factor or factors involved.

DCCOR assumes a THDA of 9.5 since this is the average THDA of all SWP images ever taken with IUE. However, the mean THDA for the images processed after 1984 for both λ Lep and ζ Cas are on average greater than this. To test if this might be the cause of the trend THDA versus radial velocity were plotted for both stars (Figures 40 and 41). From the plots it is clear that there is no correlation between THDA and radial velocity.

Throughout this report it has been noted that the radial velocities derived from LWP images are higher than they should be. These results are summarized in Table X.

Table X

Star	Average LWP RV	Average SWP RV or Known RV	Delta RV (k/s)
λ Lep	+26.0	+7.1	18.9
ζ Cas	+8.9	-8.4	17.3
RR Tel	-46.0	-61.8	15.8
HD 144579	-44.5	-60.0	15.5
HD 171232	-21.0	-35.9	14.9

Therefore, radial velocities derived from LWP images are $\sim$ 16 km/sec greater than the known radial velocities for a given system or the radial velocities derived from SWP images of the same star.

From this study the following conclusions can be made:

• There is no correlation between radial velocities measured from absorption lines present in LWP images and the dates on which the images were processed

• On average, radial velocities from derived LWP images are $\sim$ 16 km/sec higher than expected

• There does appear to be a correlation between processing date and radial velocities measured from lines present in SWP images. However, this trend does not seem to start until after June 20, 1984 when the second to last dispersion constants were implemented. This is when a second order time correction was first applied to the SWP dispersion constants. The radial velocities increase by $\sim 1.9 \pm .3$ km/sec/year

• The correlation between processing date and radial velocity appears to be due in part to the second order time correction. However, even after this has been corrected for the radial velocities are still increasing by $\sim 0.9 \pm .2$ km/sec/year

References

Bohlin,R.*et al.*,1983,ApJS,51,277.

Heckathorn,J.N.,IUE Users' Committee Meeting,Sept 1983, Appendix H.

Garhart.M.P.,1991,IUE NASA Newsletter, No.46,31.

Hoffleit,D.1982,**The Bright Star Catalogue**,New Haven,Yale University Observatory.

McNamara,D.H.,and Hansen,K.1961,ApJ,134,207.

Nichols-Bohlin,J.N.,and Fesen,R.A.1986,AJ,92,642.

Nichols-Bohlin,J.N.,and Fesen,R.A.1990,ApJ,353,281.

Nichols-Bohlin,J.N.1992,private communication.

Stickland,D.J.,1989,IUE Three-Agency Coordination Meeting, November 15,F-71.

Thompson,R,1983,IUE NASA Newsletter, No.21,39.

Thompson,R,1988a,IUE NASA Newsletter, No.35,108.

Thompson,R,1988b,IUE NASA Newsletter, No.35,133.

Thompson,R,1990,IUE NASA Newsletter, No.42,63.

Thompson,R,Bohlin,R.C.,Turnrose,B.E,and Harvel,C.A,1980,IUE NASA Newsletter, No.11,10.

Thompson,R,and Turnrose,B,E,1983,IUE NASA Newsletter, No.20,34.

Thompson,R,Turnrose,B.E,and Bohlin,1982,A & A,107,11.

Uesugi,A.1982,Revised Cat. of Stellar Rotational Velocities,Kyoto,Department of Astronomy,Kyoto U.

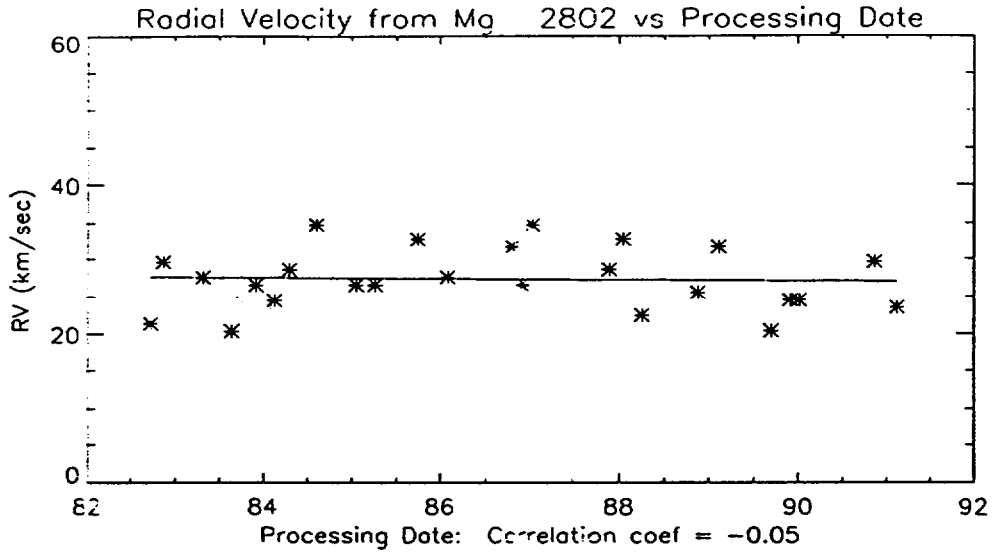

Figure 1: λ Lep: Absorption line measured with FEATURE

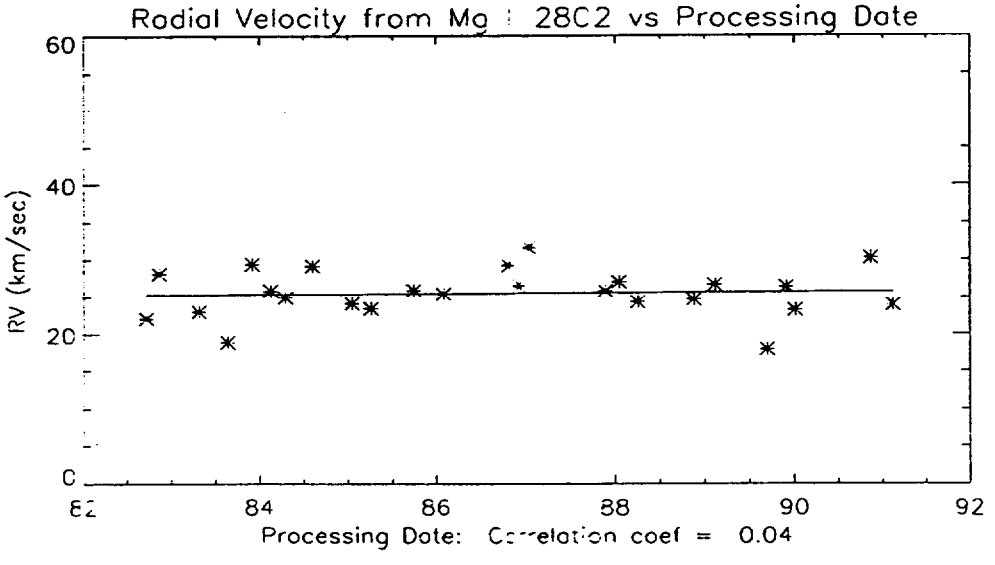

Figure 2: λ Lep: Absorption line measured with GAUSSFITS

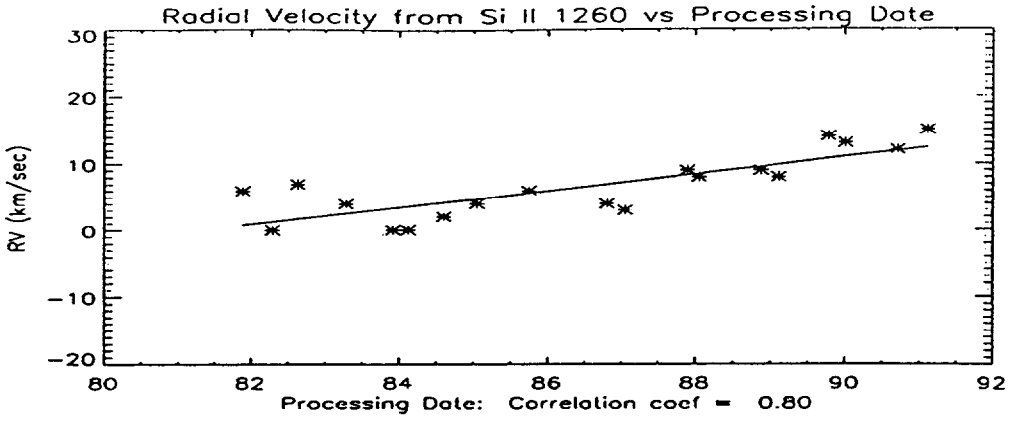

Figure 3: λ Lep: Absorption line measured with GAUSSFITS

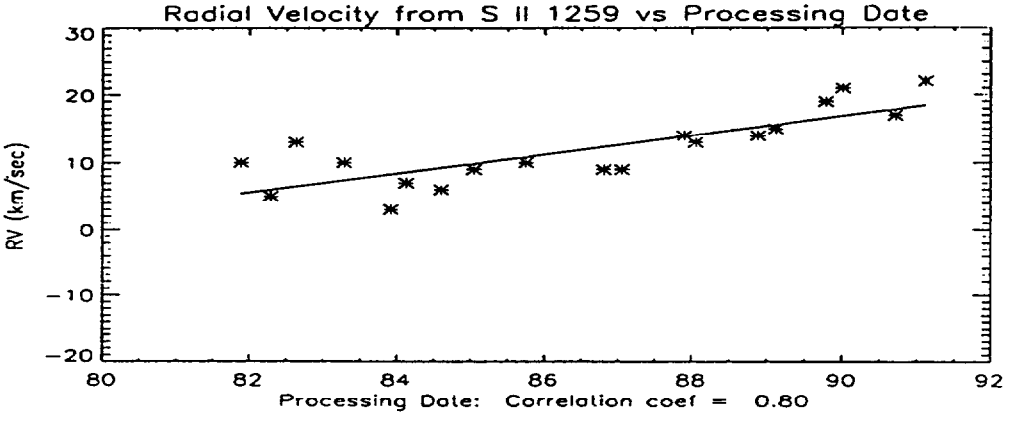

Figure 4: λ Lep: Absorption line measured with GAUSSFITS

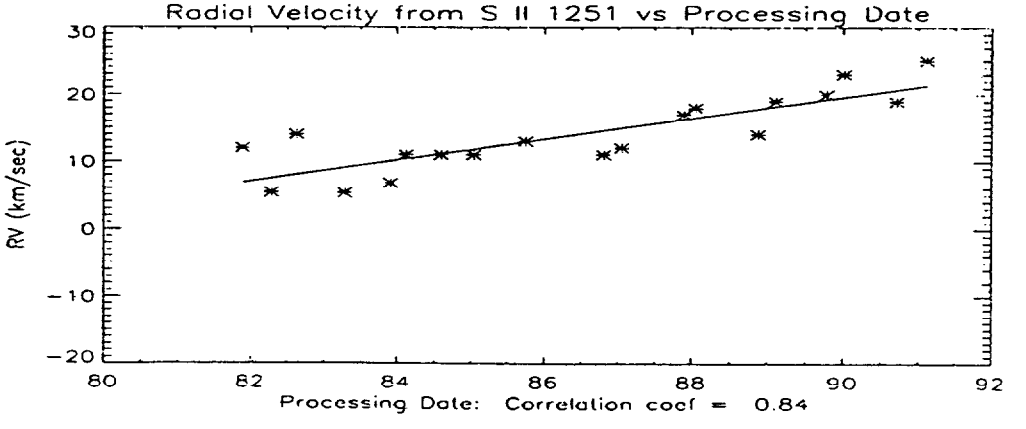

Figure 5: λ Lep: Absorption line measured with GAUSSFITS

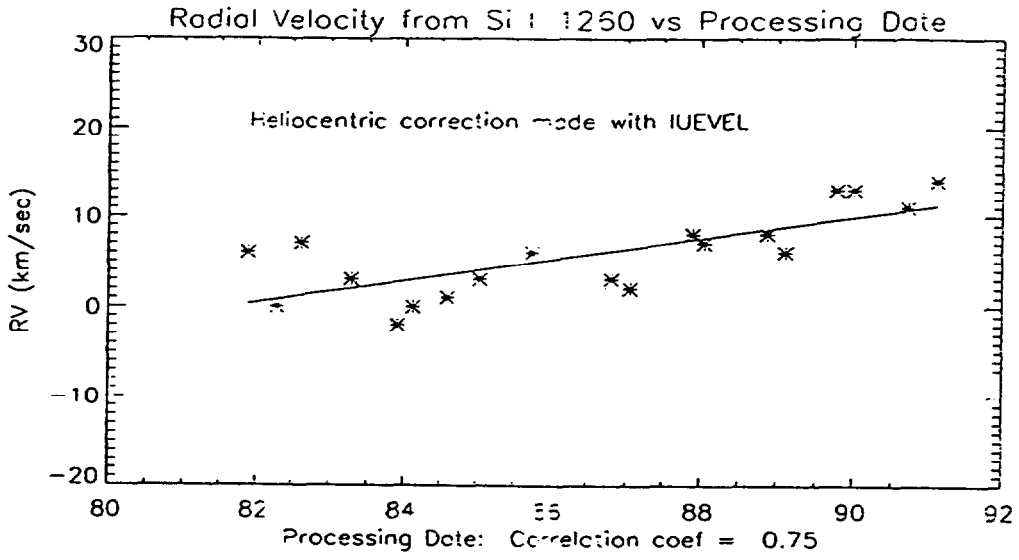

Figure 6: λ Lep: Absorption line measured with GAUSSFITS

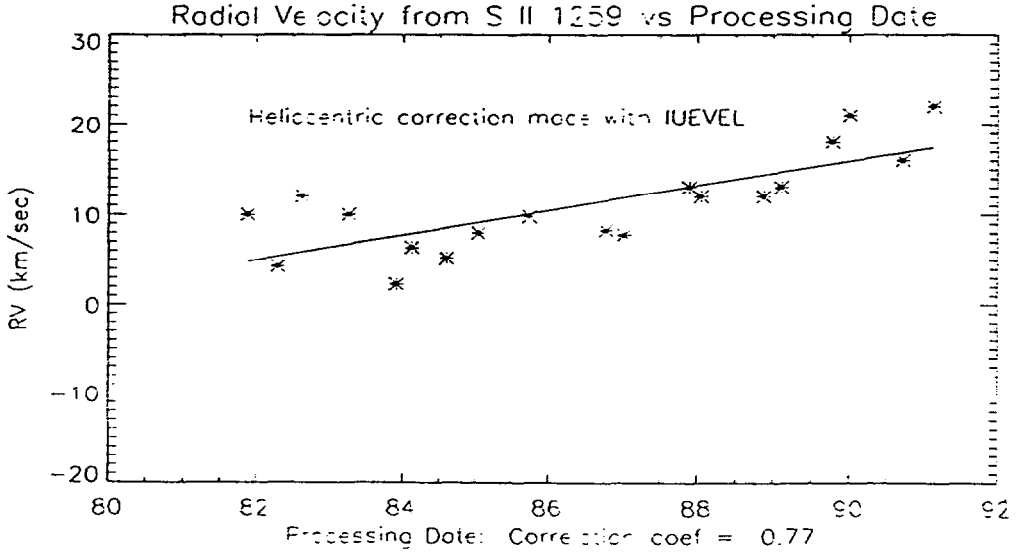

Figure 7: λ Lep: Absorption line measured with GAUSSFITS

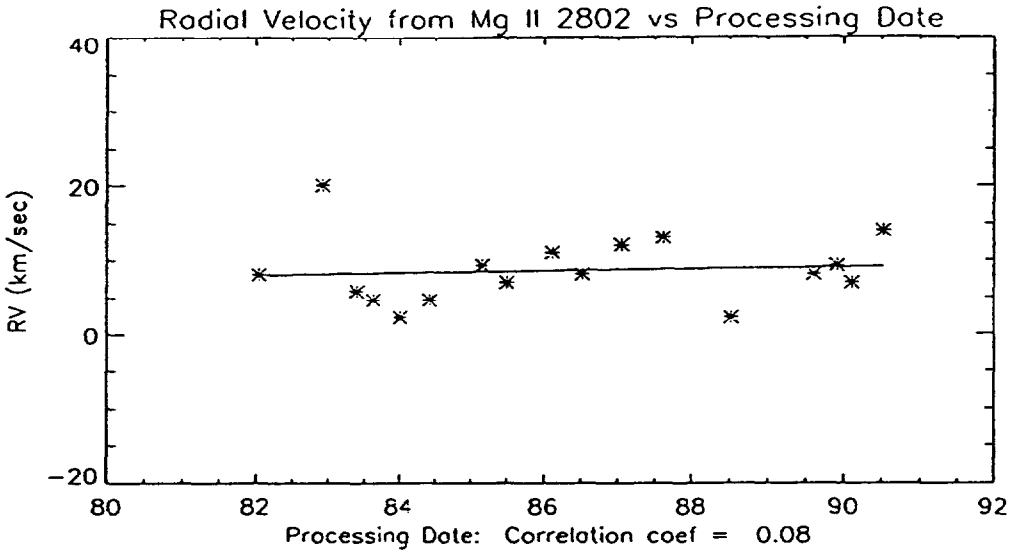

Figure 8: ζ Cas: Absorption line measured with FEATURE

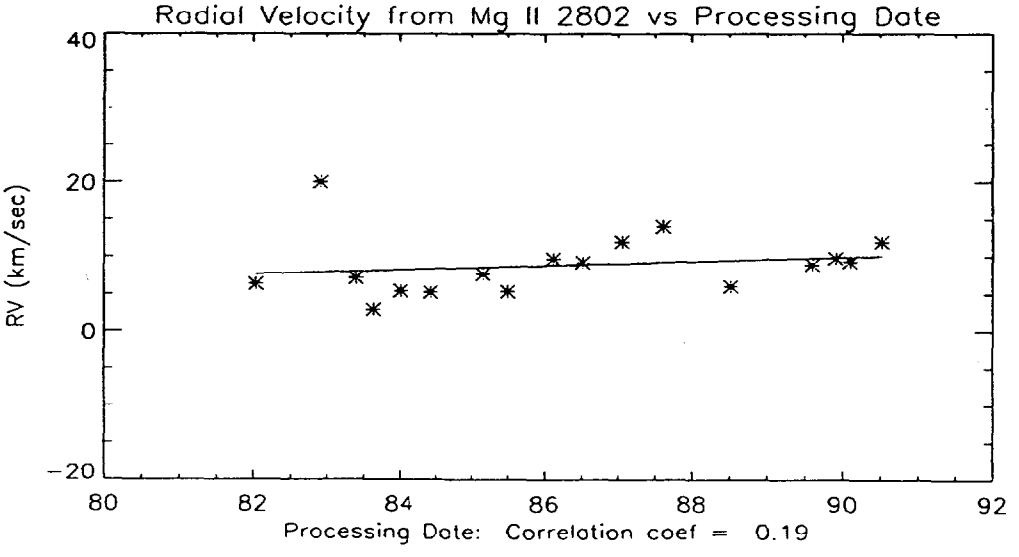

Figure 9: ζ Cas: Absorption line measured with GAUSSFITS

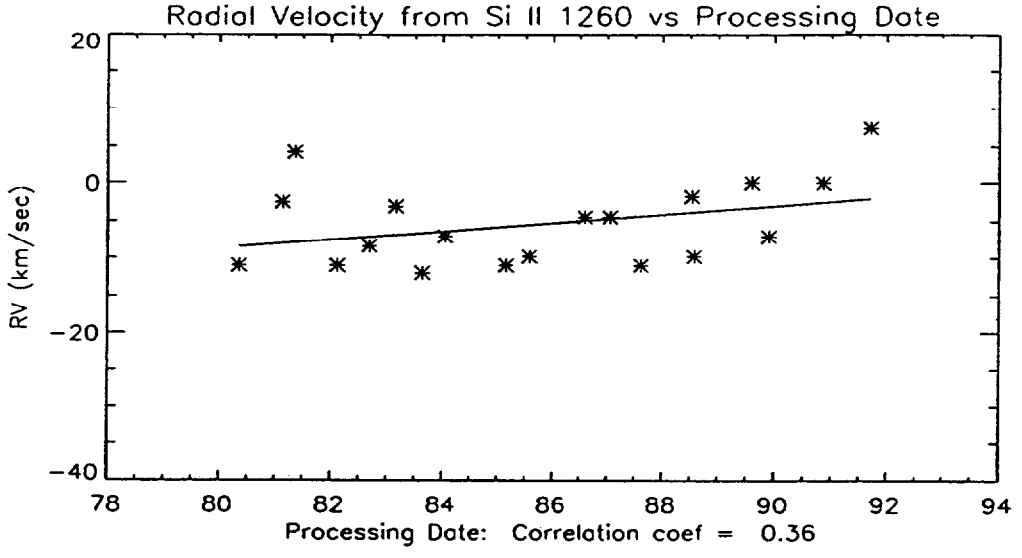

Figure 10: ζ Cas: Absorption line measured with FEATURE

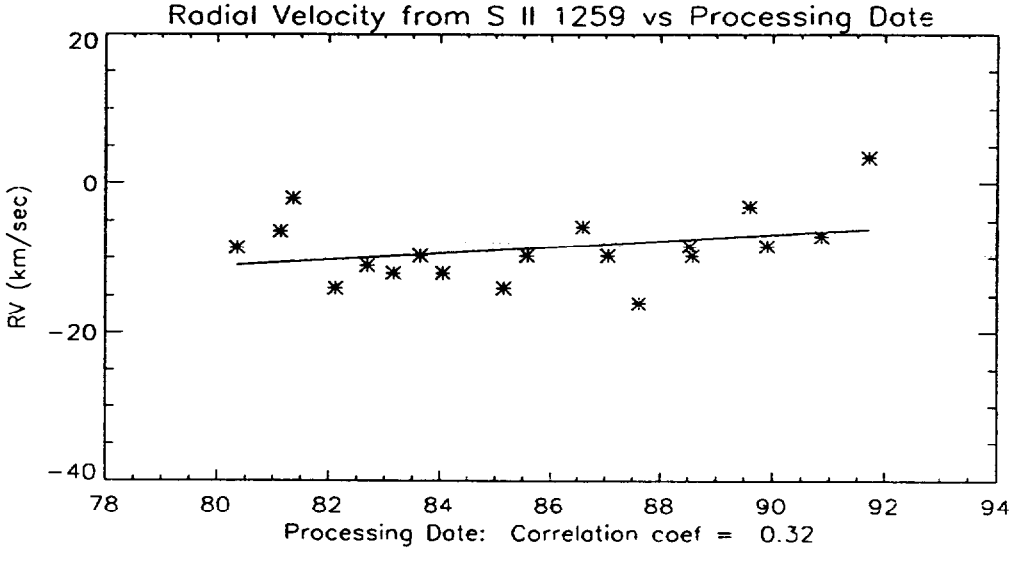

Figure 11: ζ Cas: Absorption line measured with FEATURE

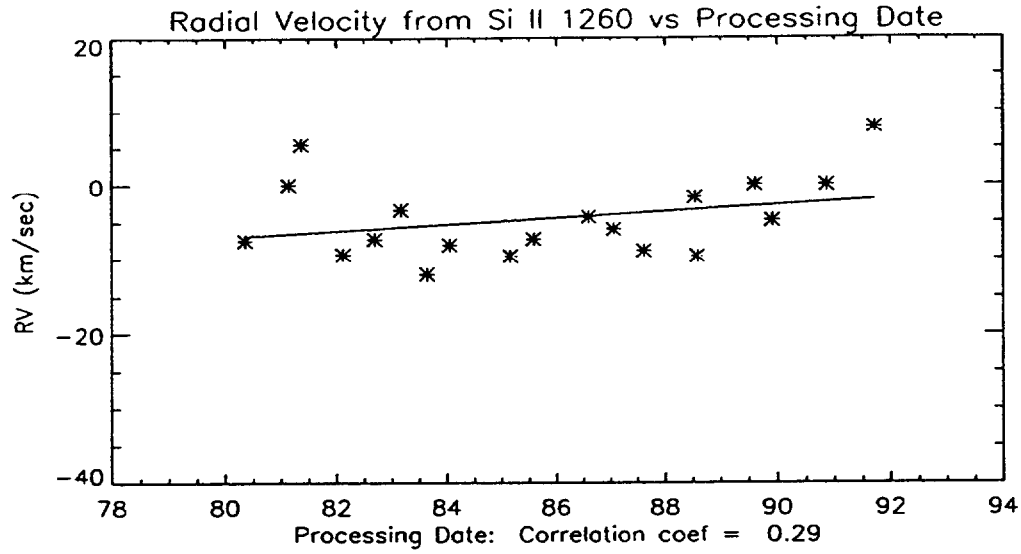

Figure 12: ζ Cas: Absorption line measured with GAUSSFITS

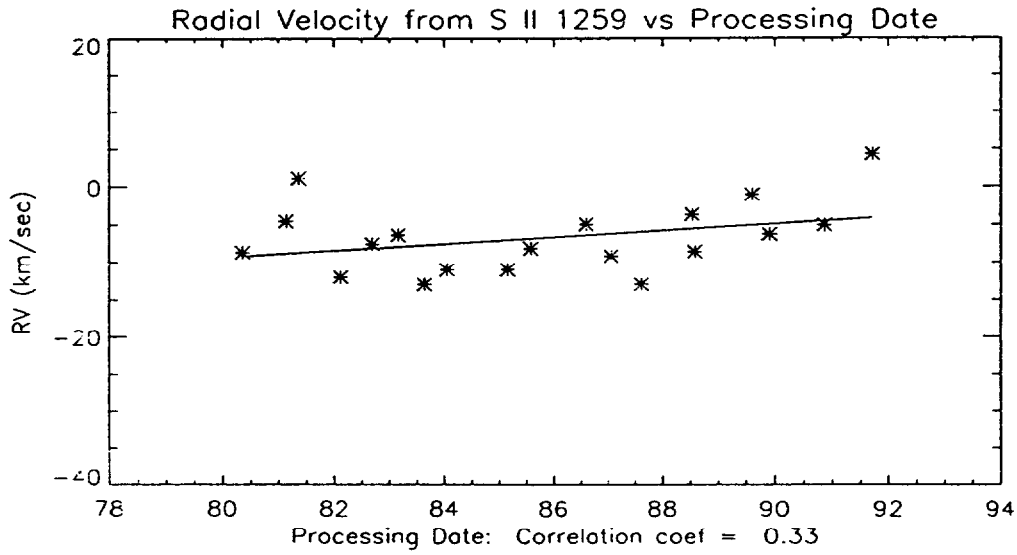

Figure 13: ζ Cas: Absorption line measured with GAUSSFITS

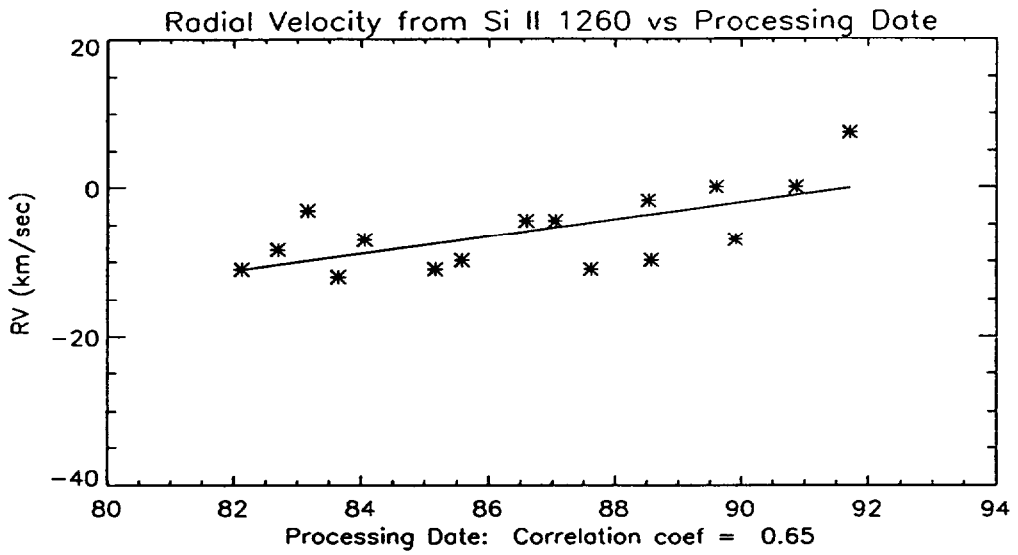

Figure 14: ζ Cas: Absorption line measured with FEATURE. Only images processed after 11/10/81 are included in the fit.

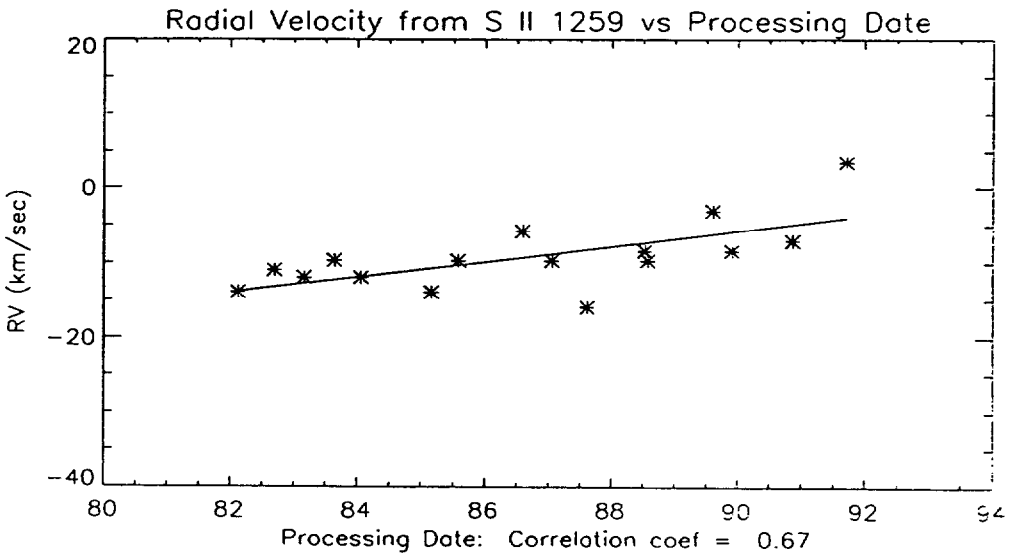

Figure 15: ζ Cas: Absorption line measured with FEATURE. Only images processed after 11/10/81 are included in the fit.

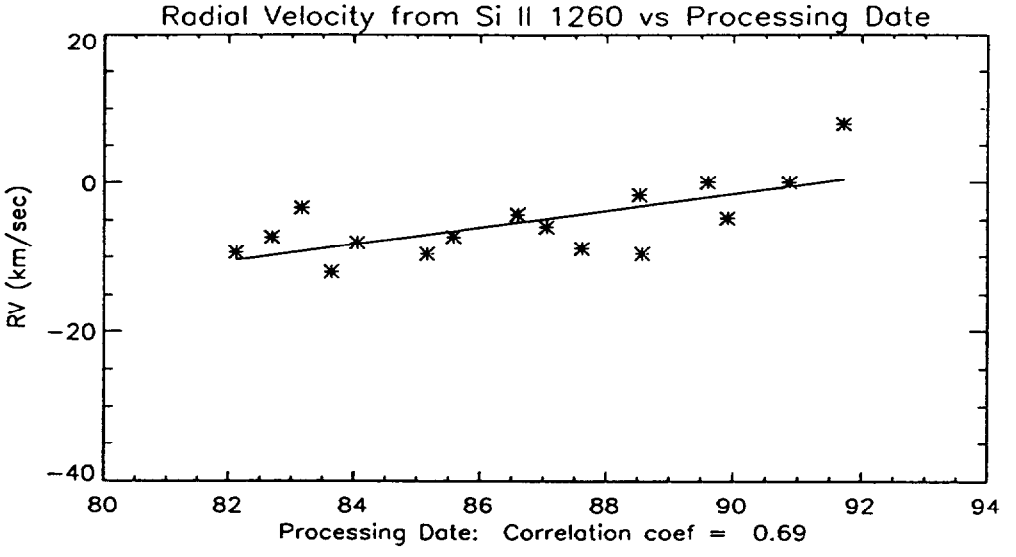

Figure 16: ζ Cas: Absorption lines measured with GAUSSFITS. Only images processed after 11/10/81 are included in the fit.

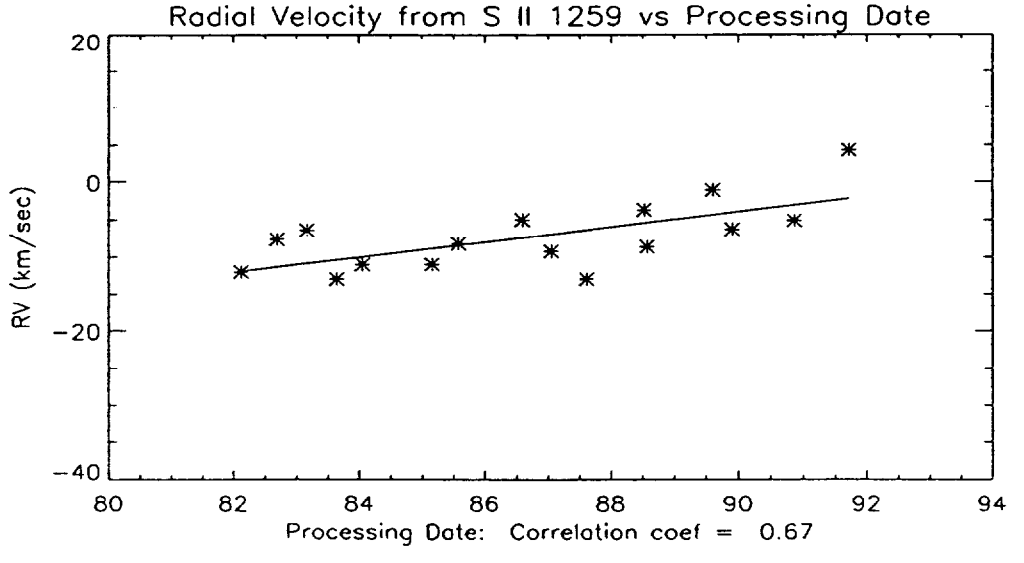

Figure 17: ζ Cas: Absorption lines measured with GAUSSFITS. Only images processed after 11/10/81 are included in the fit.

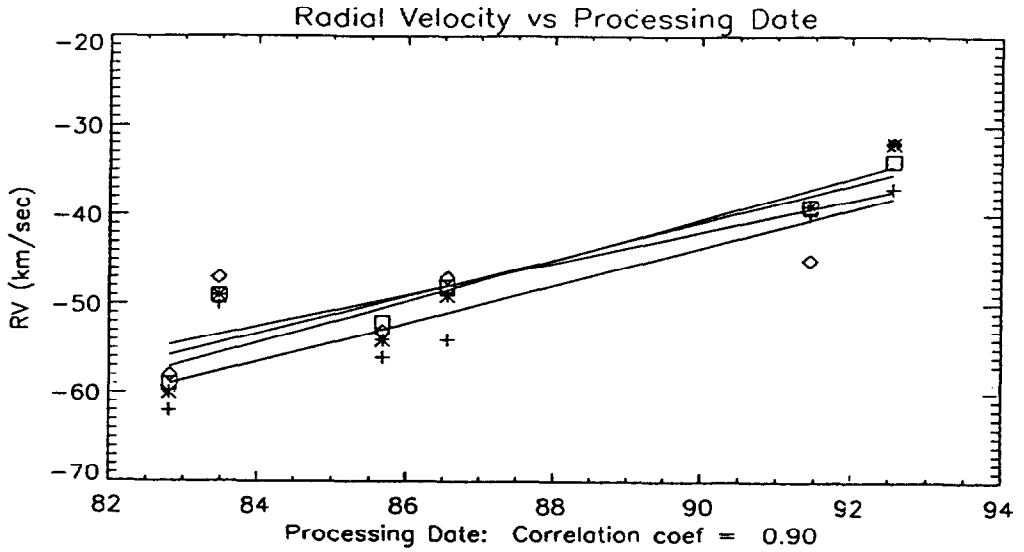

Figure 18: RR Tel: Emission lines measured with GAUSSFITS. + N IV 1243, * Si IV 1394, ◇ Si IV 1403, □ C IV 1551

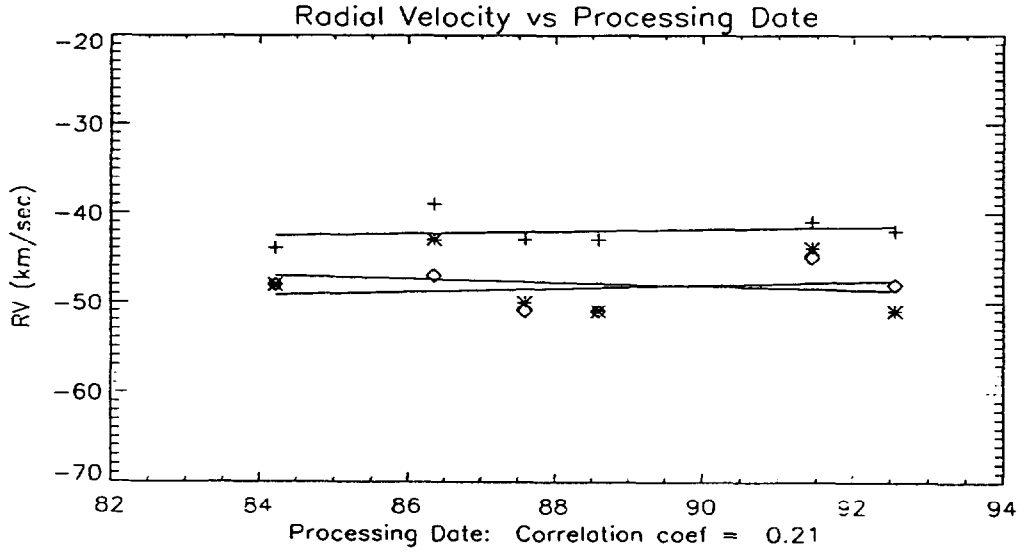

Figure 19: RR Tel: Emission lines measured with GAUSSFITS. + He II 2733, * He II 1394, ◇ Fe II 2508

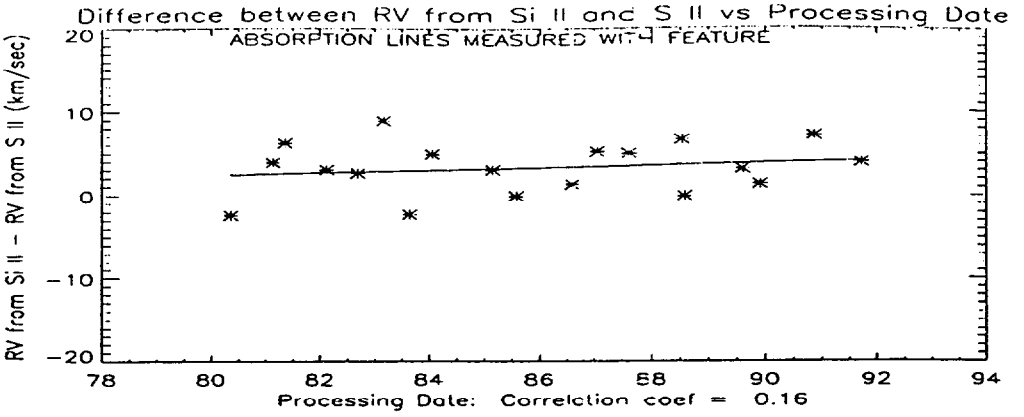

Figure 20: ζ Cas: Absorption lines measured with FEATURE.

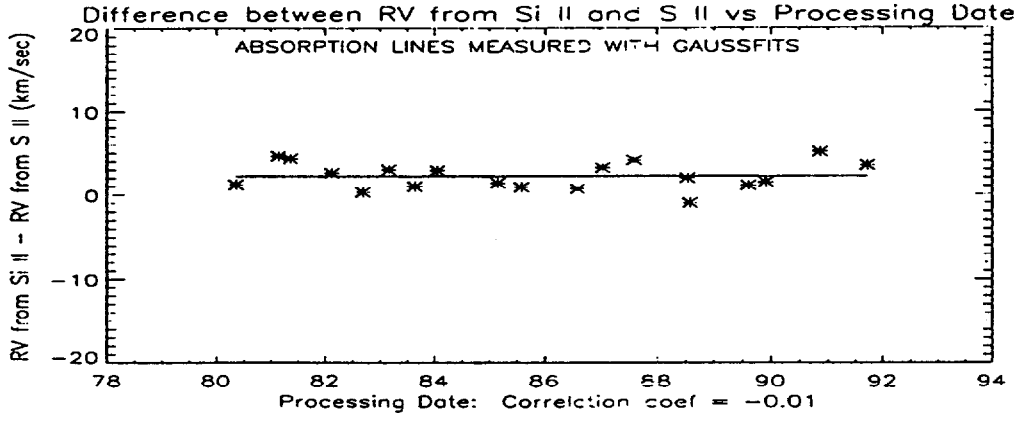

Figure 21: ζ Cas: Absorption lines measured with GAUSSFITS.

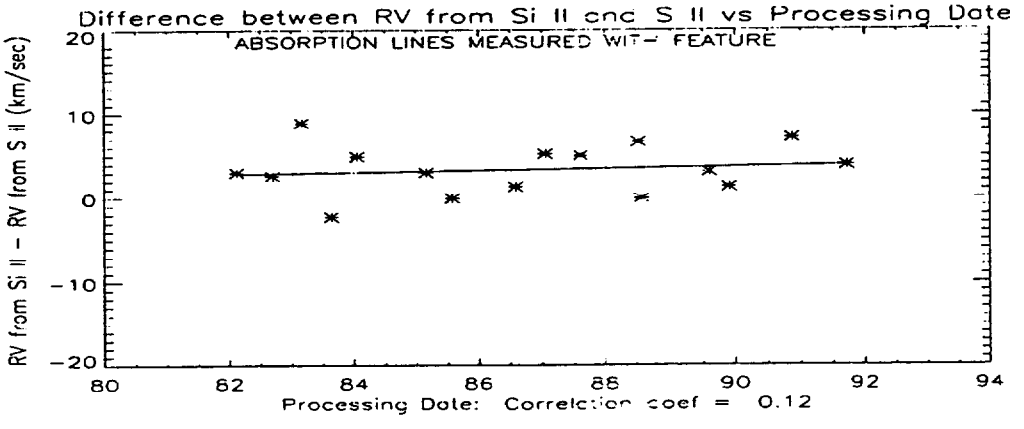

Figure 22: ζ Cas: Absorption lines measured with FEATURE. Only images processed after 11/10/81 are included in the fit.

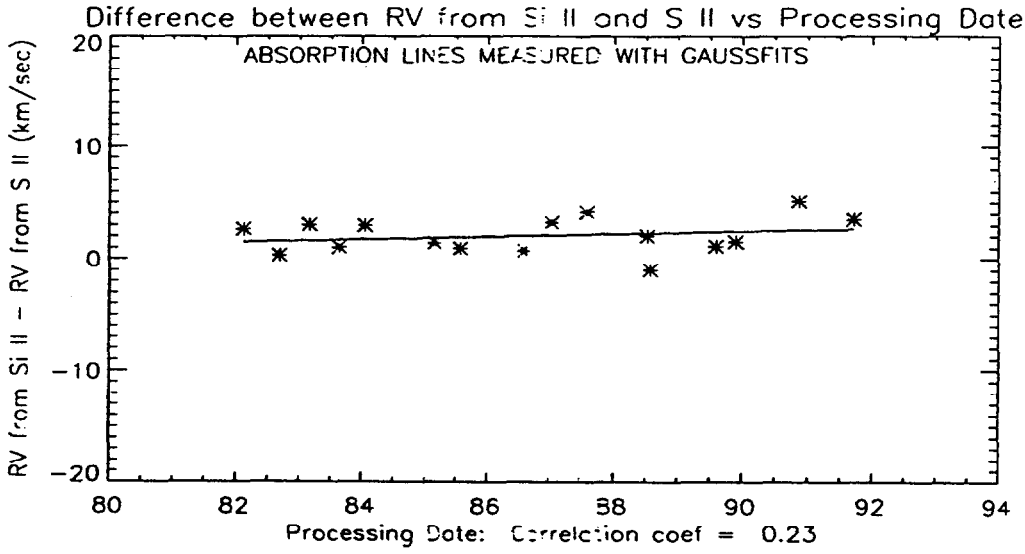

Figure 23: ζ Cas: Absorption lines measured with GAUSSFITS. Only images processed after 11/10/81 are included in the fit.

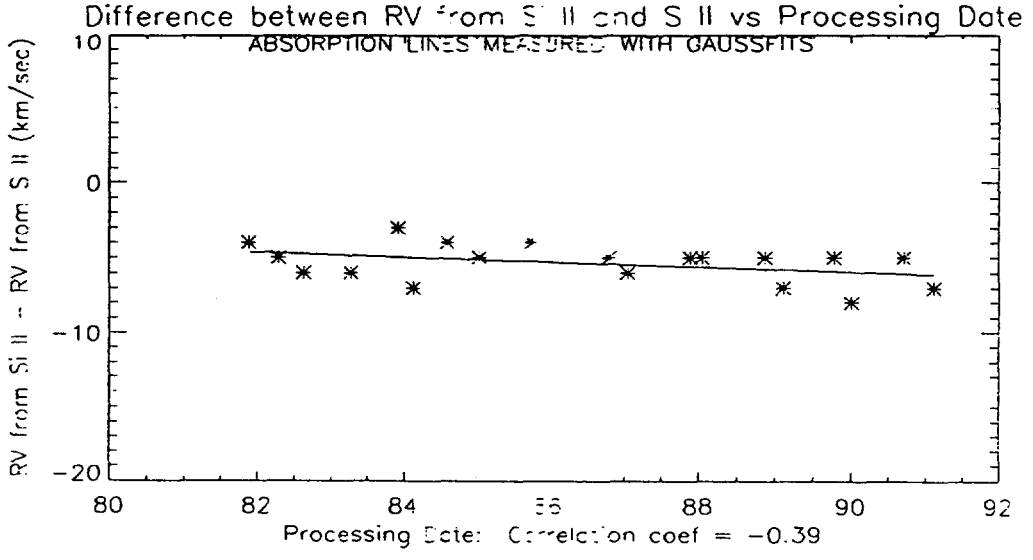

Figure 24: λ Lep: Absorption lines measured with GAUSSFITS.

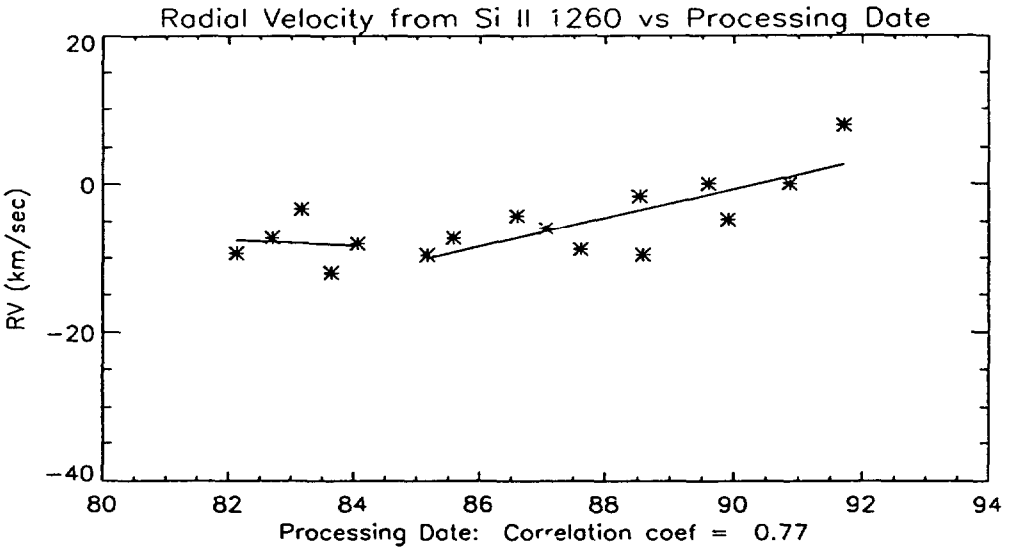

Figure 25: ζ Cas: Absorption lines measured with GAUSSFITS. Images processed between 11/10/81 and 6/20/84 are included in the first fit. Only images processed after 6/20/84 are included in the second fit.

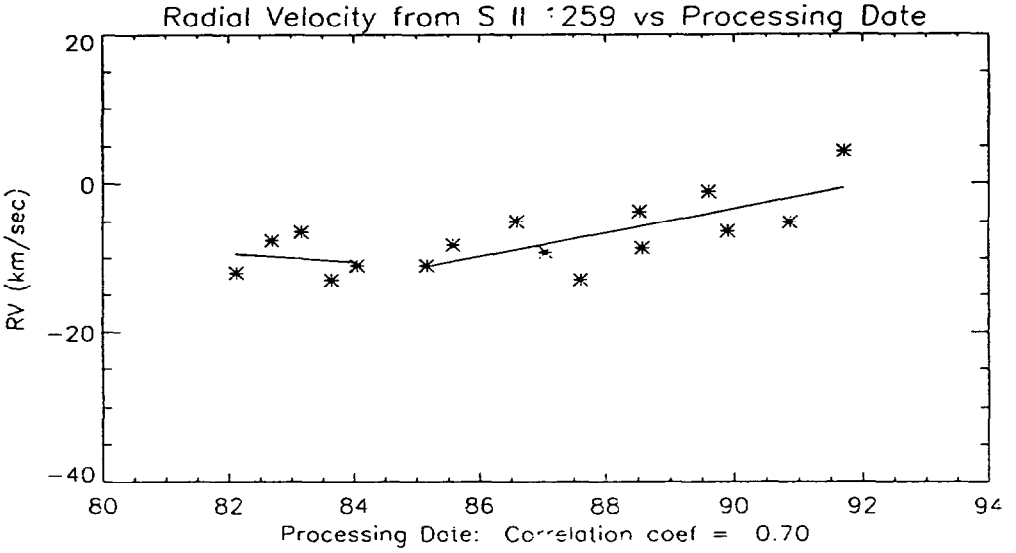

Figure 26: ζ Cas: Absorption lines measured with GAUSSFITS. Images processed between 11/10/81 and 6/20/84 are included in the first fit. Only images processed after 6/20/84 are included in the second fit.

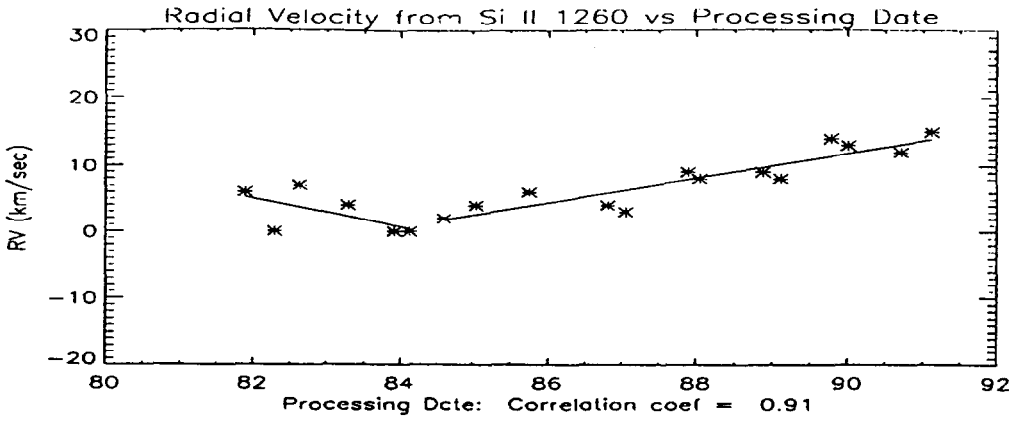

Figure 27: λ Lep: Images processed between 11/10/81 and 6/20/84 are included in the first fit. Only images processed after 6/20/84 are included in the second fit.

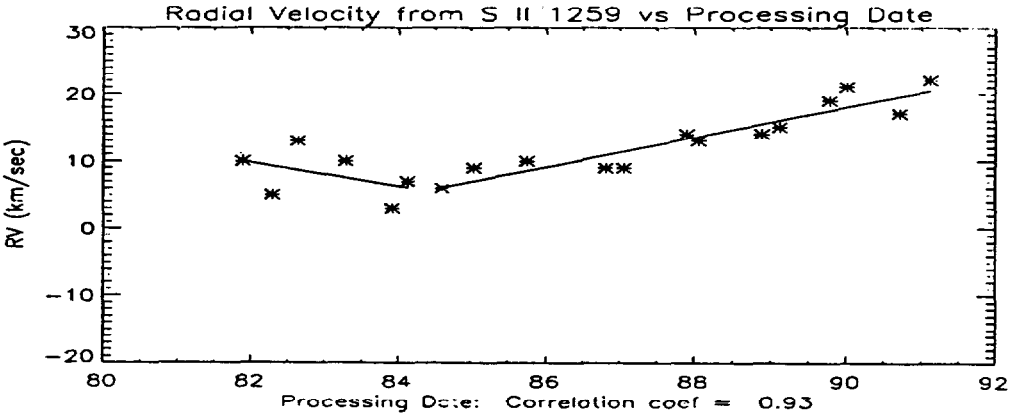

Figure 28: λ Lep: Images processed between 11/10/81 and 6/20/84 are included in the first fit. Only images processed after 6/20/84 are included in the second fit.

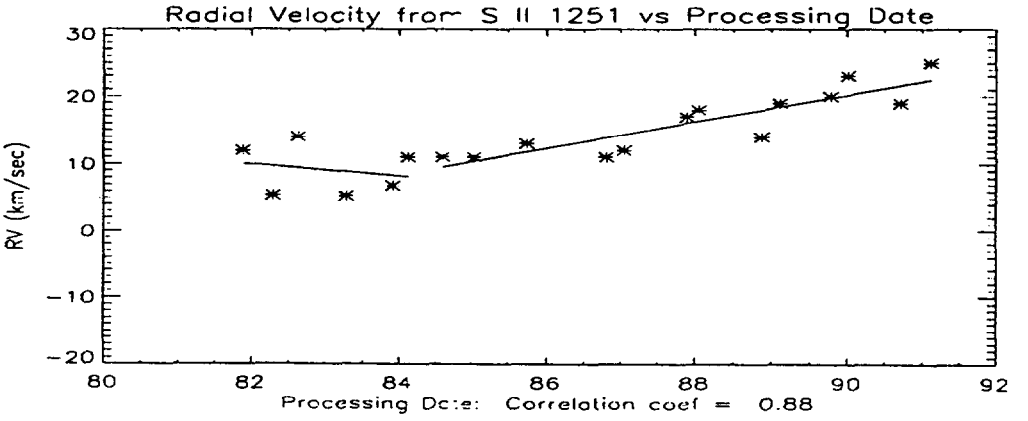

Figure 29: λ Lep: Images processed between 11/10/81 and 6/20/84 are included in the first fit. Only images processed after 6/20/84 are included in the second fit.

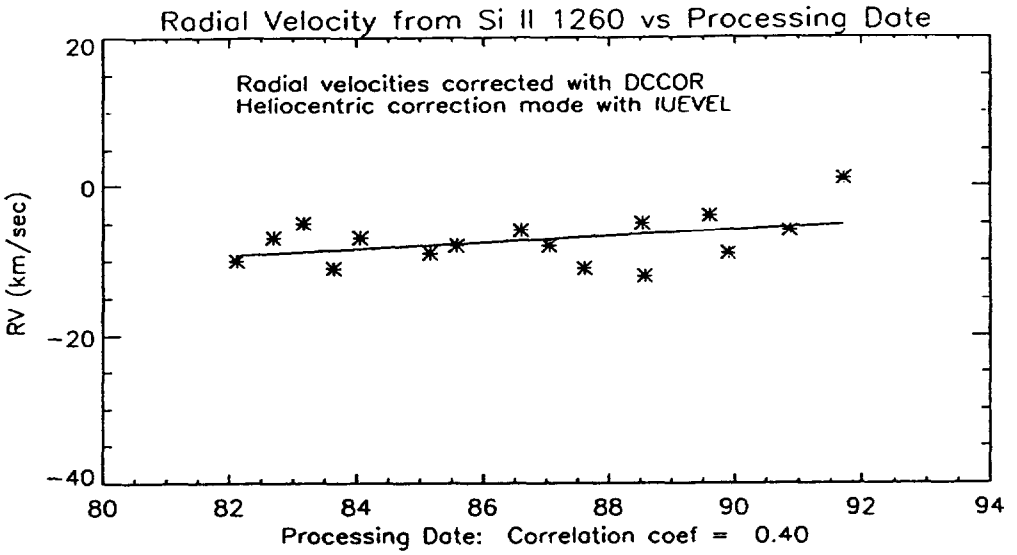

Figure 30: ζ Cas: Absorption lines measured with GAUSSFITS.

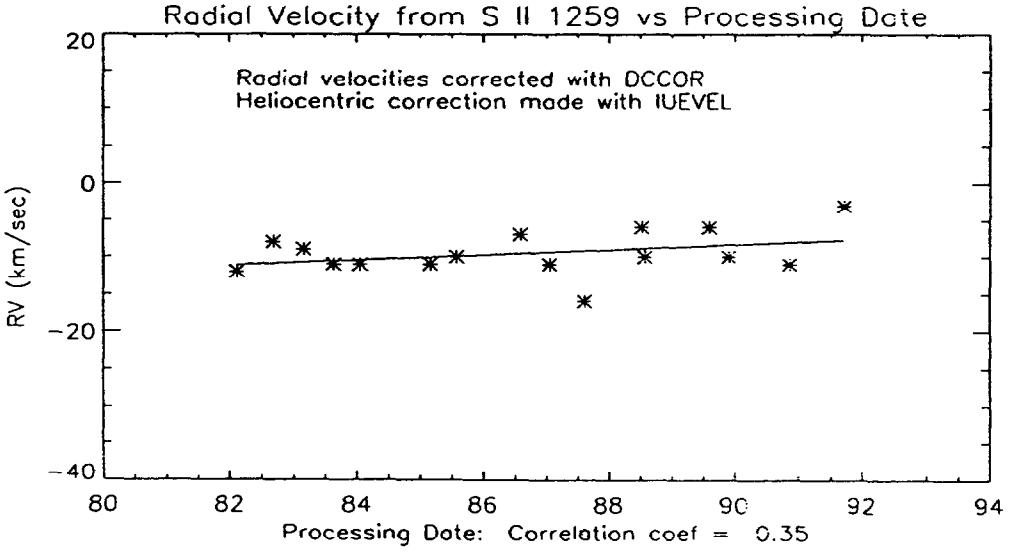

Figure 31: ζ Cas: Absorption lines measured with GAUSSFITS.

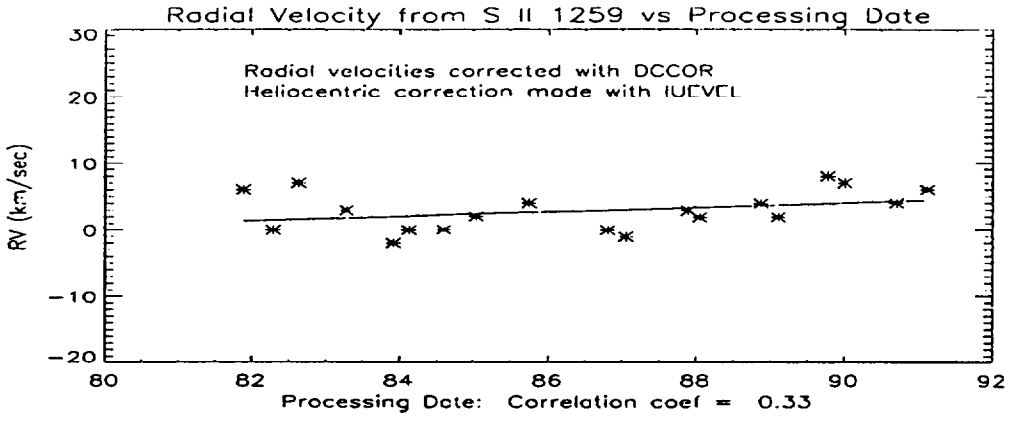

Figure 32: λ Lep: Absorption lines measured with GAUSSFITS.

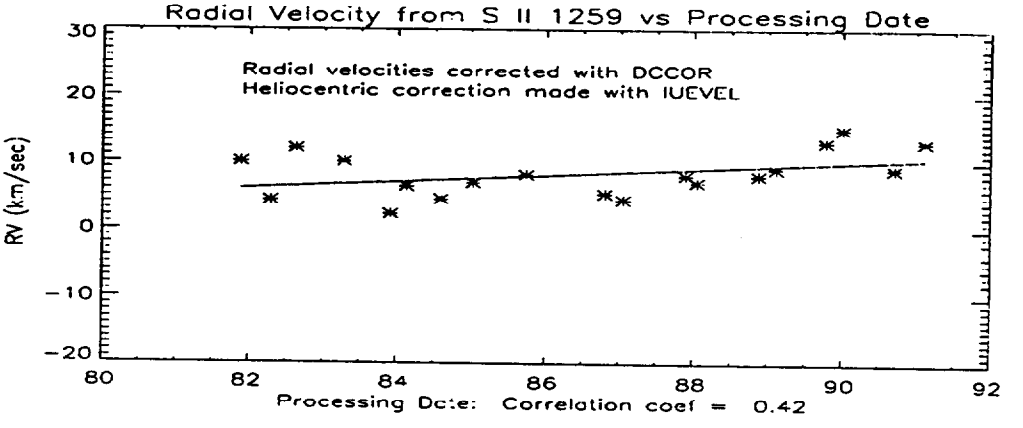

Figure 33: λ Lep: Absorption lines measured with GAUSSFITS.

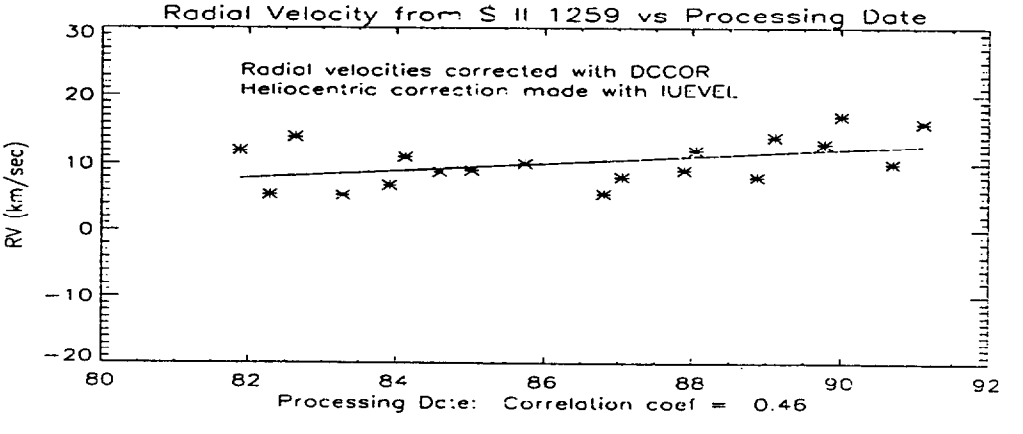

Figure 34: λ Lep: Absorption lines measured with GAUSSFITS.

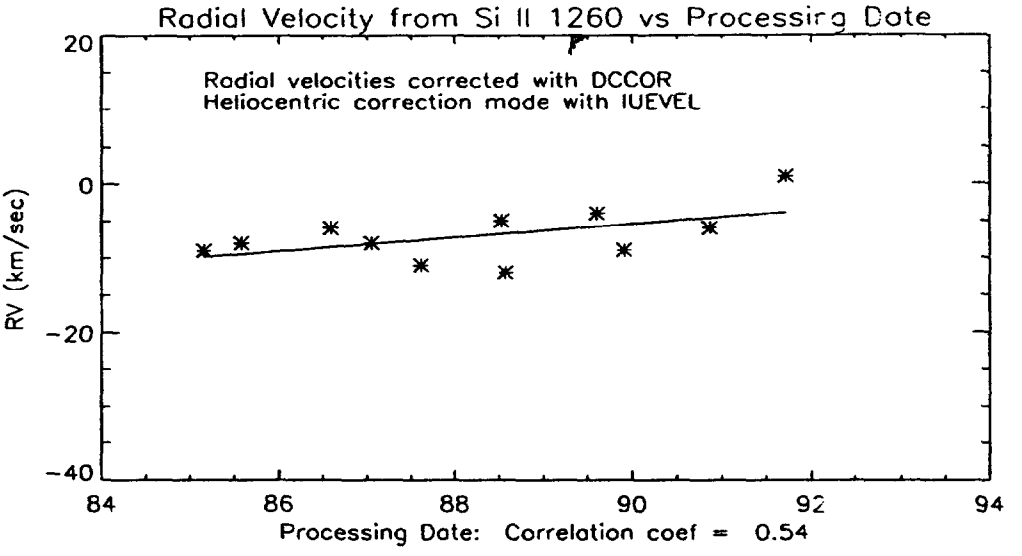

Figure 35: ζ Cas: Absorption lines measured with GAUSSFITS. Only images processed after 6/20/84 are included in the fit.

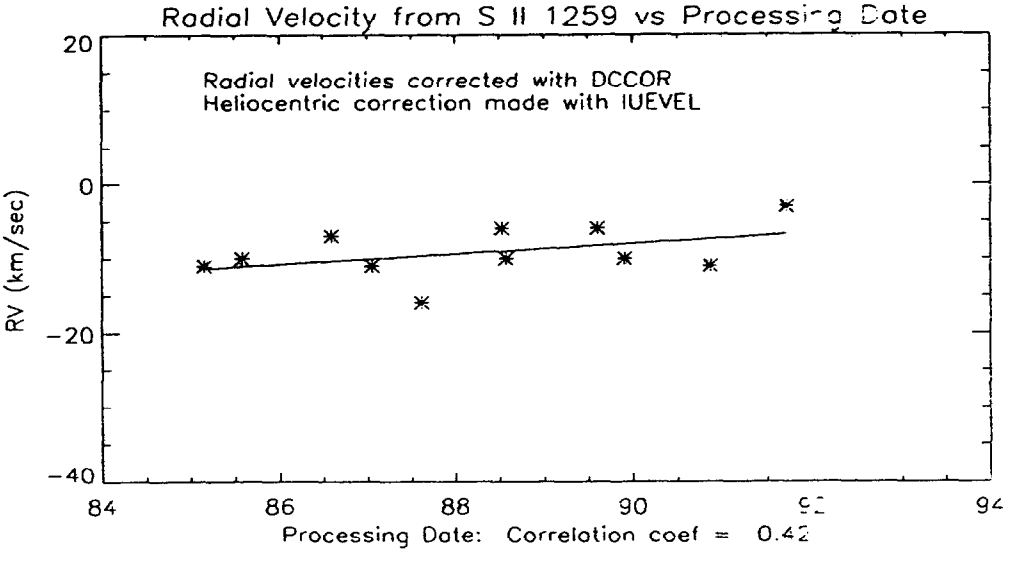

Figure 36: ζ Cas: Absorption lines measured with GAUSSFITS. Only images processed after 6/20/84 are included in the fit.

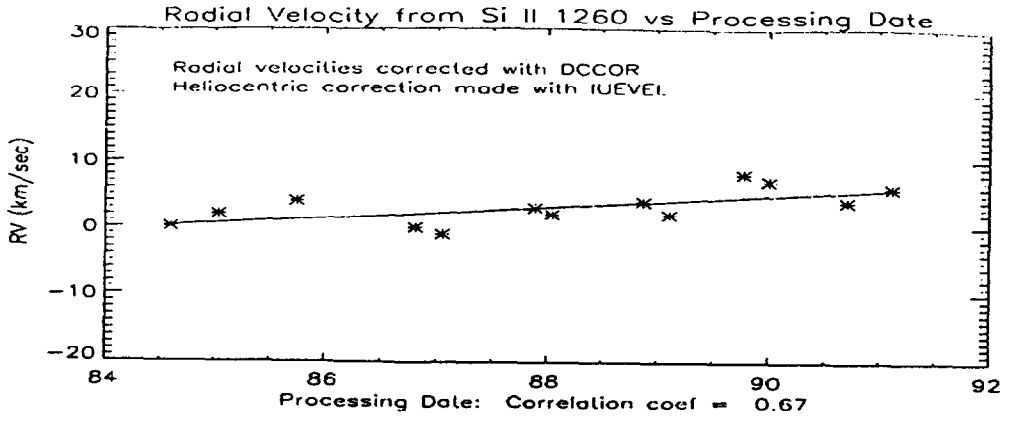

Figure 37: λ Lep: Absorption lines measured with GAUSSFITS. Only images processed after 6/20/84 are included in the fit.

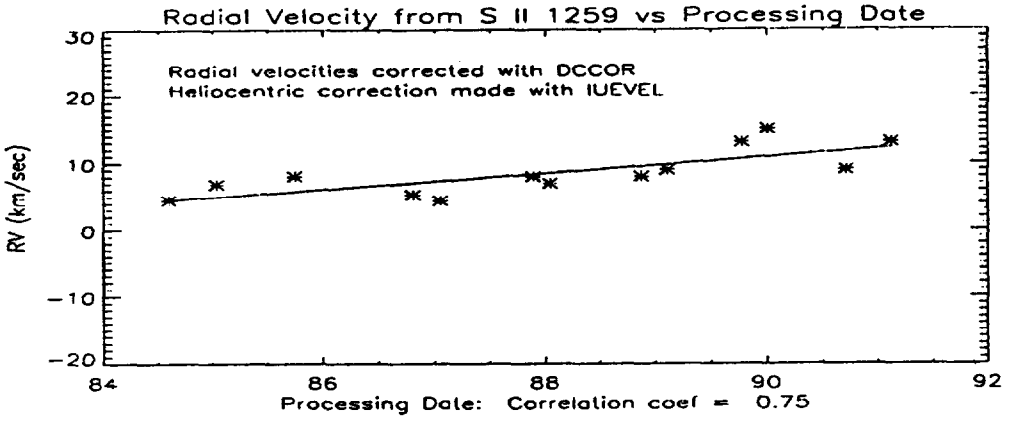

Figure 38: λ Lep: Absorption lines measured with GAUSSFITS. Only images processed after 6/20/84 are included in the fit.

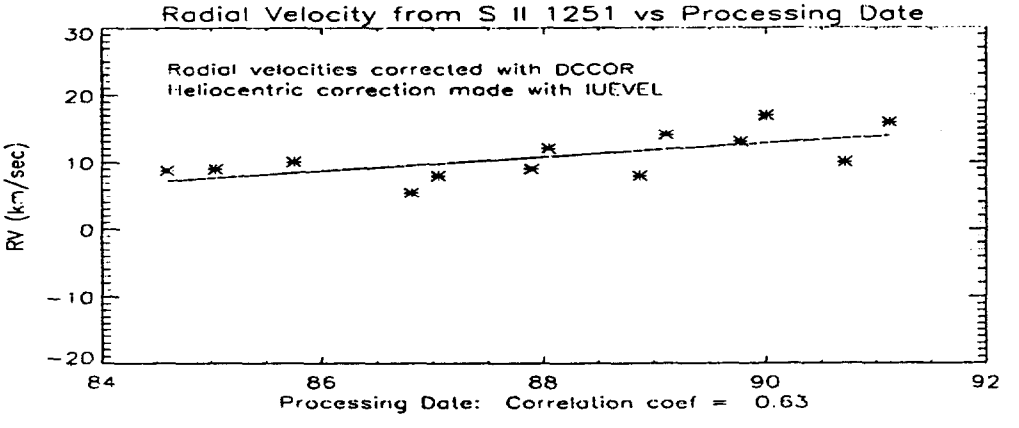

Figure 39: λ Lep: Absorption lines measured with GAUSSFITS. Only images processed after 6/20/84 are included in the fit.

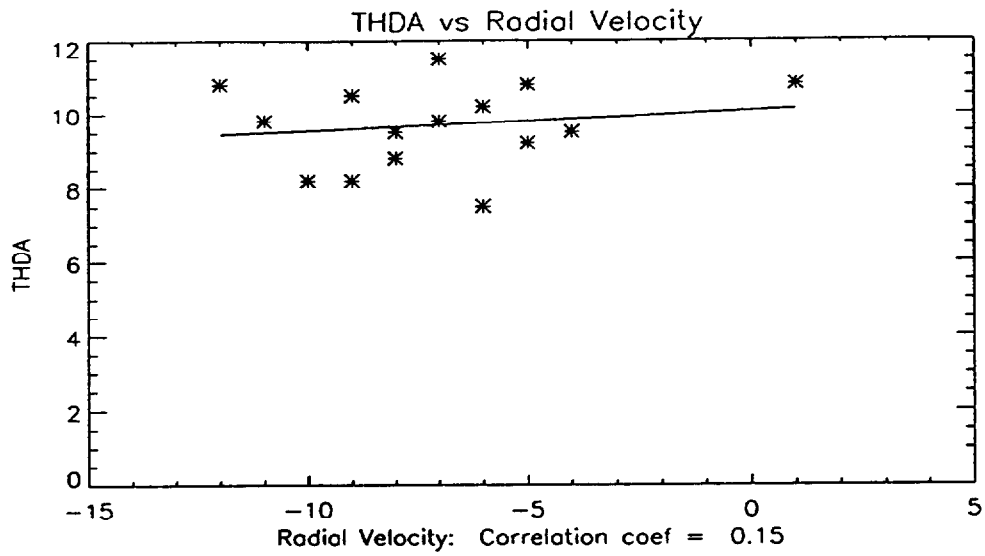

Figure 40: ζ Cas: Absorption lines measured with GAUSSFITS.

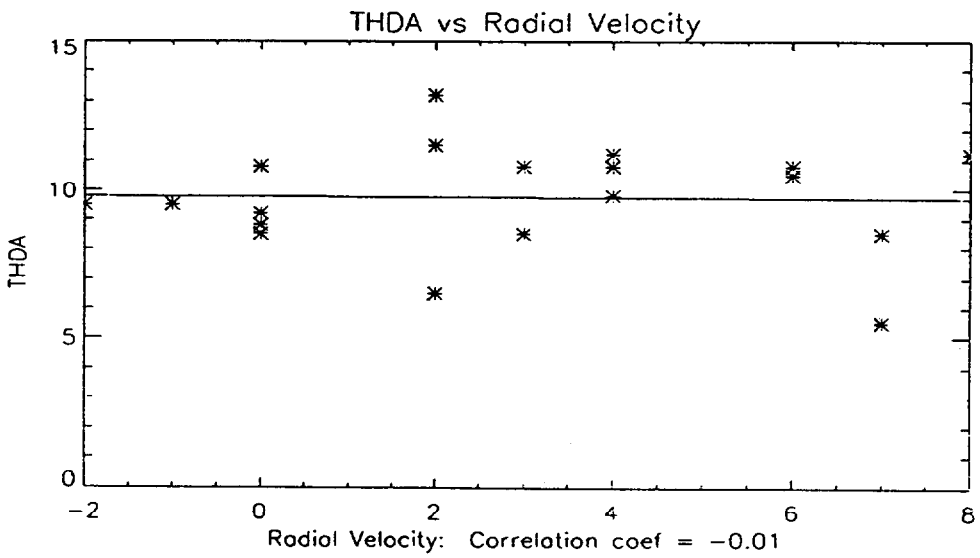

Figure 41: ζ Cas: Absorption lines measured with GAUSSFITS.